Published in IET Renewable Power Generation
Received on 27th February 2007
Revised on 10th September 2007
doi: 10.1049/iet-rpg:20070012

ISSN 1752-1416

Introducing a coloured fluid stochastic Petri net-based methodology for reliability and performance evaluation of small isolated power systems including wind turbines

Y.A. Katsigiannis P.S. Georgilakis G.J. Tsinarakis

Department of Production Engineering and Management, Technical University of Crete, Chania 73100, Greece
E-mail: katsigiannis@dpem.tuc.gr

Abstract: A new approach in reliability evaluation of small isolated hybrid power systems, which include wind turbines and conventional generators, based on fluid stochastic Petri net (PN) modelling is presented. A major novelty of the proposed methodology is that a selection of constant time intervals is adopted, instead of assuming continuous dynamics. The proposed analysis presents similar characteristics with simulation methods, with the additional advantages of graphical representation of system's components and attributes. Moreover, emphasis is given on the parameterisation of input data that describes operational and reliability characteristics of the system, so a global investigation of the examined system can be done. In order to import more precise data in the simulation process modelled by the PN, the concept of database arcs is introduced. The evaluation is based on the calculation of system's basic indices related to reliability estimation and energy production. The results obtained verify the flexibility and the capabilities of the proposed methodology.

Nomenclature

SIPS	small isolated power systems
RES	renewable energy sources
CDG	conventional diesel generator
WT	wind turbine
PN	Petri net
CPN	coloured Petri net
FSPN	fluid stochastic Petri net
CFSPN	coloured fluid stochastic Petri net
LOLP	loss of load probability
LOLE	loss of load expectation
LOEE	loss of energy expectation
EIU	energy index of unreliability
SI	severity index
FOI	frequency of interruptions
DOI	duration of interruptions
ENSI	energy not supplied index
LCI	load curtailment index
WEP	wind energy produced
CEP	conventional energy produced from CDG
CF	capacity factor
SE	surplus energy
SFSPNm	subnet of fluid stochastic Petri net model
MTTF	mean time to failure
MTTR	mean time to repair
TTF	time to failure
TTR	time to repair
P	set of FSPN places
P_d	subset of FSPN discrete places
P_c	subset of FSPN continuous places

T	set of FSPN transitions
T_e	subset of FSPN stochastically timed transitions
T_i	subset of FSPN immediate transitions
A	set of FSPN arcs
A_n	subset of FSPN normal arcs
A_i	subset of FSPN inhibitor arcs
A_t	subset of FSPN test arcs
A_{db}	subset of FSPN database arcs
B	function that describes the upper bound of tokens on each FSPN place
W	weight function that refers to FSPN arc multiplicity weights
M_0	initial state of FSPN
$\boldsymbol{p}_i$	place i of FSPN
$\boldsymbol{t}_i$	transition i of FSPN
$\boldsymbol{M}_{Pi}$	marking of place $\boldsymbol{p}_i$
Σ	finite set of non-empty types, also called colour sets, of a CPN
C	colour function that is defined from the set of places P to Σ
G	guard function that maps each transition into a Boolean expression where all variables have types that belong to Σ
C	continuous FSPN place
D	discrete FSPN place
P_R	rated power of WT
V_{in}	cut-in speed of WT
V_{out}	cut-out speed of WT
R^2	R^2 coefficient of determination
P_{WT}	WT generated power
V	wind speed
z_{hub}	hub height of WT
z_{anem}	anemometer height
a	power-law exponent
$V(z_{hub})$	wind speed at hub height
$V(z_{anem})$	wind speed at the anemometer height
rnd(0, 1)	uniformly distributed random number generation function in the interval (0, 1)

1 Introduction

Small isolated power systems (SIPS) provide electricity supply in remote areas that cannot be economically connected to the electrical grid. In such areas, renewable energy sources (RES) are usually present in large amounts, so RES technologies can be used as a supplementary energy source working in parallel with conventional diesel generators (CDGs) in order to save fuel. Wind turbines (WTs) are the primary choice of RES technologies in such systems, as they can provide large amounts of energy, they have reduced costs compared with other RES technologies, they require reasonable maintenance and there is no fuel cost. However, the nature of wind is intermittent, so wind penetration cannot be large, in order to ensure an acceptable reliability level of the system.

For the reliability evaluation of SIPS, mainly deterministic techniques have been applied [1]. However, these techniques do not define consistently the true risk of the system, as they can lead to very divergent risks even for systems that are very similar [2]. In addition, these techniques cannot be extended to include intermittent sources, such as wind energy [3]. Besides the deterministic techniques, the other two basic approaches for reliability evaluation of power systems are the direct analytical methods and the Monte Carlo simulation. Most of the published work in SIPS that contain wind-energy conversion systems is focused on the use of analytical methods [4] which, however, cannot recognise completely the chronological variation of wind and its effect in the operation of SIPS that include WTs.

Petri nets (PNs) are a graphical and mathematical tool, originally developed for the analysis of discrete event systems. Extension of their use for dynamic systems modelling made necessary the introduction of time delays, leading to the definition of (deterministic) timed PNs and stochastic PNs [5]. Moreover, the high complexities of such systems guide to high-level abbreviations in the original graphical representation of PNs. Coloured PNs (CPNs) [6] belong to this category, because with the use of colours, they allow more compact representation of complicated models. This simplifies significantly the modelling of certain complex systems while maintaining at the same time the discrete character of the tool. To enhance the application of PNs in the field of continuous systems, several extensions and variations were introduced, such as hybrid PNs [7, 8] and fluid stochastic Petri nets (FSPNs) [9]. These PN types at the same time include both continuous and discrete components, and thus they can describe hybrid systems, such as power systems.

In this paper, the choice of coloured FSPNs (CFSPNs) as modelling and evaluation tool has been made because of the characteristics of the considered problem. In particular, the need for CPNs can be justified from the existence of repeated net structures in the overall model considered. Using CPNs reduces significantly the overall model complexity and simplifies its analysis and further study. In contrast, FSPNs have been selected, since they concentrate on the evolution of

IET Renew. Power Gener., 2008, Vol. 2, No. 2, pp. 75–88

doi: 10.1049/iet-rpg:20070012

the stochastic process involved [10]. In the system considered, there exists a large number of continuous variables (e.g. power output), some of which are stochastic, as well as they take only discrete values (e.g. hours of the year). As a result, the PN variation that combines all the desired characteristics is CFSPNs.

In the power system area, PNs have been used for reliability evaluation and fault diagnosis, mainly in transmission and distribution systems [11, 12]. In power generation, PNs have been used in the analysis of grid-connected systems [13, 14] and isolated systems [15]. However, both types of systems described contain only conventional energy sources, so modelling of RES technologies seems to be a new task.

This paper proposes a reliability and performance evaluation methodology for SIPS based on FSPNs, using a novel approach: instead of assuming continuous dynamics defined by the change of fluid level over time as in literature, a selection of constant time intervals has been adopted here, and the most important quantitative and qualitative characteristics of system's operation are studied. The examined SIPS may include one or more WTs and one CDG, and the calculations are done on an hourly basis. The hourly values of load consumption and wind speed are inserted in the proposed FSPN using the database arcs that are introduced in this paper. A major advantage of the proposed methodology is that the PN model is very flexible, since several of its variables are parameterised. Another benefit is that it can be treated in two ways: as a typical simulation procedure and a combination of graphical and mathematical representation of SIPS operation state at each hour of the simulation. Thus, the proposed methodology can be used either by SIPS planners and designers for the evaluation of different system configurations or by SIPS operators for the simulation of system's operation and the examination of system's performance under several operating states including extraordinary conditions.

2 Reliability and performance evaluation of SIPS

For the considered SIPS, the load demand is assumed to follow the hourly chronological shape of the IEEE-RTS [16] with a peak load of 20 kW. Two types of power-generation components have been considered: (1) WTs with 20 kW rated power and (2) CDGs with 15 kW rated power. The number of CDGs is kept constant and equal to one, as multiple-diesel strategies are normally applied in much larger isolated systems [17], whereas the number of WTs can vary from one to three. The evaluation of each examined system is based on the calculation of nine reliability (indices 1–9) and four performance indices (indices 10–13) [2]:

1. loss of load probability (LOLP);

2. loss of load expectation (LOLE), expressed in h/year;

3. loss of energy expectation (LOEE), expressed in kW h/year;

4. energy index of unreliability (EIU), which normalises LOEE by dividing it with the annual energy demand;

5. severity index (SI), expressed in system min/year;

6. frequency of interruptions (FOI), expressed in int/year;

7. duration of interruptions (DOI) that is equal to LOLE/FOI, expressed in h/int;

8. energy not supplied index (ENSI) that is equal to LOEE/FOI, expressed in kW h/int;

9. load curtailment index (LCI) that is equal to LOEE/LOLE, expressed in kW/int;

10. wind energy produced (WEP), expressed in kW h;

11. conventional energy produced (CEP) from CDG, expressed in kW h;

12. capacity factor (CF);

13. Surplus energy (SE),

expressed in kW h, which is produced from the power generation components of the system, but it cannot be utilised for satisfying the load demand. It can be used for regulation of system's frequency, for applications such as space or water heating and water purification, or it can be dissipated [18].

3 Fluid stochastic PNs

The FSPNs used in this paper arise from the FSPN definition presented in [19], by adapting some of their features according to the desired behaviours. An FSPN is defined as FSPN $= \{P, T, A, B, W, M_0\}$, where P is the set of places partitioned into the subset of discrete places P_d and the subset of continuous places P_c and T is the set of transitions partitioned into the subset of stochastically timed transitions T_e and the subset of immediate transitions T_i. The set A of arcs is partitioned into four subsets: the subset A_n of normal arcs, the subset A_i of inhibitor arcs, the subset A_t of test arcs and the subset A_{db} of database arcs. In a PN, transitions and places are connected through arcs

interchangeably. Function B describes the upper bound of tokens on each place. The weight function W refers to arc multiplicity weights and can be a constant number, a mathematical function or a function of certain places' markings. Finally, the initial state of FSPN is denoted by M_0.

In an FSPN, continuous places are drawn as double circles, discrete places as simple circles and transitions are represented as single bars. Immediate transitions are black bars and timed transitions (either deterministic or stochastic) are empty bars. In case of structural conflicts, priorities in the firing of the transitions can be defined. The default priority for a transition is 1, whereas transitions with higher priorities are represented with the typical bar symbol, containing their priority index.

Normal arcs are drawn as usual arcs, inhibitor arcs are represented by arcs whose end is marked with a small circle, whereas test arcs are represented by arcs with dotted lines. Database arcs are analytically described in Section 4. The use of inhibitor and test arcs significantly increases the modelling capabilities of a PN. If a place p and a transition t are connected with an inhibitor arc with weight w, t can only fire if the marking of p is less than w. On the contrary, if p and t are connected with a test arc with weight w, t can only fire if the marking of p is greater than or equal to w. Also when p and t are connected with a normal arc with weight w, t can only fire if the marking of p is greater than or equal to w. The major difference is that firing a transition subtracts w tokens when p and t are connected with normal arcs, whereas no token movement takes place through inhibitor and test arcs.

In FSPNs, the study of hybrid system's continuous part is performed by assuming rates equal to arc weights that connect continuous places and timed transitions. The product of arc's weight with the time duration of its related transition is equal to the fluid level change. However, in SIPS simulation models (such as HOMER [20] and HYBRID2 [21]), constant time intervals – mainly hourly – are considered, and during them the input and output variables of the system are supposed to be constant. The operation of the proposed FSPN follows this approach. Places are used to calculate the main characteristics of SIPS operation. Continuous places are used to calculate variables taking the real numbers as values, whereas discrete places are used to calculate of variables taking the positive integers as values, as well as for the control of transitions firings. In the whole PN model, there is only one timed transition with duration equal to the selected time interval. The remaining transitions are immediate and the simulation exploits the structural PN properties of concurrency and parallelism to proceed. Arc weights are used to calculate the characteristics studied and quite often their value is a function of a place marking.

The combination of continuous places with immediate transitions is not used in classical FSPNs, as it results in an event that keeps reoccurring with probability equal to one. In the approach followed here, this problem can be solved by adding a discrete place as an additional input to the immediate transition. Fig. 1 presents a simple example that is equivalent to an IF statement. The presence of one token in discrete place p_2 is essential for firing once the transition that satisfies the true condition. For markings of p_1 less than 5 (that is the arc weight of the inhibitor arc), t_2 fires, whereas for markings of p_1 greater than or equal to 5 (that is the arc weight of the test arc), t_1 fires. The symbol M_{Pi} related to certain arcs denotes that these arc weights are equal to the marking of place p_i.

The formal definition of CPNs adds into the tuple of an ordinary PN the quantities Σ, C and G. More specifically, Σ is a finite set of finite and non-empty types, also called colour sets; C is a colour function that is defined from the set of places P to Σ and G is a guard function that maps each transition into a Boolean expression where all variables have types that belong to Σ.

4 Database arcs

In a PN simulation, some variables represented by places may have to take specific values that either cannot be modelled in a PN environment or their modelling will increase significantly the graphical complexity of the system. For example, in order to examine the performance of a SIPS for a specific hourly load profile of a year (8760 values), large numbers of places and arcs must be added to the PN to obtain the desired load value for each hour. To reduce the consequences of such problems, the concept of database arcs is introduced in this paper. A database

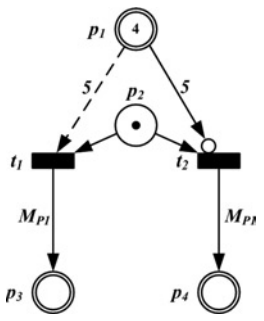

Figure 1 *Implementation of IF condition using inhibitor and test arcs*

doi: 10.1049/iet-rpg:20070012

arc is a directed arc from a transition (immediate or timed) to a continuous or discrete place whose weight can take values that are contained in a given matrix $\boldsymbol{A}$. It is symbolised as an arc that contains square brackets together with the name of the input matrix. The markings of transitions' input places give the position of the element in $\boldsymbol{A}$ that is desirable to be imported in the considered analysis. These places are of discrete type; they can enable the transition if their markings are greater than zero, and after the firing process, their marking becomes zero. A transition can fire again only if all of its input places are re-filled.

Fig. 2 shows an example of graphical modelling and operation of a database arc. In this example, the database arc is considered to obtain values from matrix $\boldsymbol{A}$

$$\boldsymbol{A} = \begin{bmatrix} 2 & 12.6 & -4 \\ -10.56 & 198 & 7 \\ -\sqrt{3} & 0 & \exp(2) \end{bmatrix} \quad (1)$$

The correspondence between the values of the discrete input places of a database arc and the matrix position of the element that is desirable to be imported is achieved from the information contained in the name of each discrete input place. The operation of a database arc is presented in Fig. 2, where it is desirable to import the value of a specific row (second row in this example) and a specific column (third column in this example) of the two-dimensional matrix $\boldsymbol{A}$ of (1) into the place p_1. Since matrix $\boldsymbol{A}$ is two-dimensional, two discrete input places are needed: (1) p_{1_1} to indicate the row of matrix $\boldsymbol{A}$ (where the last digit of p_{1_1}, 1, is an index that denotes the first dimension – row – of matrix $\boldsymbol{A}$) and (2) p_{1_2} to indicate the column of $\boldsymbol{A}$ (where the last digit of p_{1_2}, 2, is an index that denotes the second dimension – column – of matrix $\boldsymbol{A}$). The left part of Fig. 2 shows the state of the PN before the firing of t_1, from which it can be seen that $M_{P1\_1} = 2$ (since the place p_{1_1} has two tokens) and $M_{P1\_2} = 3$ (since the place p_{1_2} has three tokens). The right part of Fig. 2 shows the state of the PN after the firing of t_1, from which it can be seen that the place p_1 has a marking value of 7, since $\boldsymbol{A}(M_{P1\_1}, M_{P1\_2}) = \boldsymbol{A}(2,3) = 7$.

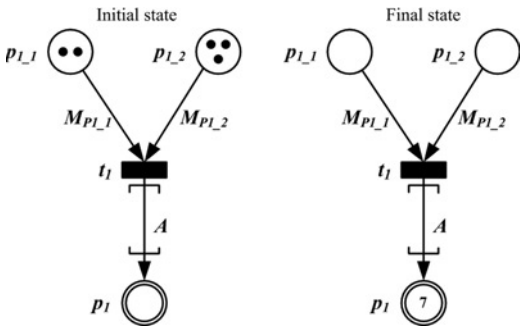

Figure 2 *Operation of database arcs*

It is possible to retrieve the desired value of a matrix by putting the appropriate marking in PN's input places. For example, the PN model can be adjusted to export sequentially the elements of a row, a column, a diagonal or to make a random selection. The use of database arcs can be very helpful in the following situations, especially when the number of data is large.

1. When it is desirable to import data that have to take specific values in a given sequence (e.g. meteorological data).

2. When the data does not follow any typical probability distribution function.

5 SIPS modelling with FSPNs

This section describes the proposed FSPN methodology that has been used for the hourly simulation of a SIPS, taking into account the load demand, the wind speed variation and WT power generation and the conventional generator operation. All the necessary simulations were implemented using visual object net PN simulation package [22].

The structure of the proposed FSPN contains five subnets of FSPNm models (sFSPNm): (1) the input layer sFSPNm that contains time information and parameter values, (2) the load demand sFSPNm that imports load data to the model, (3) the WT sFSPNm that simulates the WT operation, (4) the CDG sFSPNm that simulates the CDG operation and (5) the output layer sFSPNm that calculates reliability and performance indices. A schematic representation of

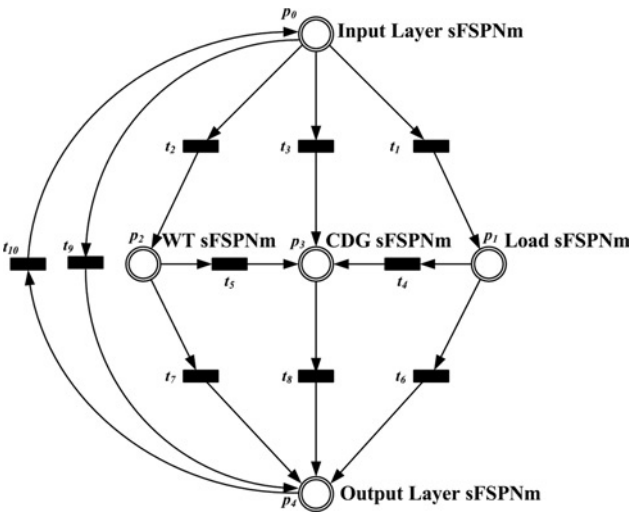

Figure 3 *Schematic representation of the overall FSPN model*

the overall model is presented in Fig. 3. Each of the depicted places represents the model of a subnet and the transitions show the interactions between them. This overall PN model is not executed, but it represents an upper hierarchy level of the system.

The three intermediate modules (load, WT and CDG) of the proposed FSPN calculate the supply and demand of energy. The load model imports load data with the help of database arcs. The WT model imports wind speed data via database arcs and implements the simulation procedure of one or more WTs of the same type. In case of existence of multiple WTs, the same CPN model is used and each WT is represented by different colours. The conventional generator model simulates the operation and maintenance of the CDG. The load and WT models are used as input to the CDG model, as the decision of whether the CDG will operate is related to the load and WT power output values of the specific hour. Although the proposed PN simulates the entire year, it can be used to examine the results for any specific period of the year (summer period, specific months or weeks and so on) with only a few modifications.

A brief description of each one of the five sFSPNm follows. For simplicity, in cases where there is a connection between sFSPNm, only their direct connected parts with the sFSPNm described are depicted.

5.1 Input layer sFSPNm

For the flexible parameterisation of the system, the input layer of the proposed FSPN contains all the values that can be modified by the user, as well as the variables describing simulation time, in order to evaluate the performance of SIPS under different conditions. The corresponding places, their description, their type [either continuous (C) or discrete (D)] and their initial values are presented in Table 1. Moreover, the input layer consists of two transitions: the immediate transition $\boldsymbol{t}_{i1}$, which is needed for the conversion of simulation years (place $\boldsymbol{p}_{i1}$) to simulation hours (place $\boldsymbol{p}_{i2}$) and the timed transition $\boldsymbol{t}_{i2}$, which represents the hourly time step of the simulation. Finally, a discrete place named $\boldsymbol{p}_{i20}$ is also contained, in order to ensure the proper firing of $\boldsymbol{t}_{i1}$.

The WT modelling is implemented using a power-curve profile that is based on manufacturer's data. The selected WT has the following characteristics: rated power P_R equal to 20 kW, cut-in speed V_{in} equal to 3 m/s and cut-out speed V_{out} equal to 24 m/s. For the WT power-curve fitting, a seventh-order polynomial expression has been selected, as it provides accurate correlation with real data ($R^2 = 99.87\%$), while it presents exclusively positive values for the generated power P_{WT} in the interval $[V_{in}\ V_{out}]$. The obtained equation is shown as

$$\begin{aligned} P_{WT}(V) = {} & 1.07 \times 10^{-6} \times V^7 - 1.20 \times 10^{-4} \\ & \times V^6 + 5.36 \times 10^{-3} \times V^5 - 0.12 \\ & \times V^4 + 1.42 \times V^3 - 8.46 \\ & \times V^2 + 24.24 \times V - 26.36 \\ & \text{for } V_{in} \le V \le V_{out} \end{aligned} \tag{2}$$

where V is the wind speed. The correlation between power curve's real and fitted data is shown in Fig. 4.

5.2 Load demand sFSPNm

To implement the load model, the imported data that consist of the values of hourly load expressed as a percentage of annual peak come from the IEEE-RTS [16], with the help of database arcs. Load for each hour is then calculated by multiplying the resulting ratio with the annual peak load demand.

5.3 Wind turbine sFSPNm

Wind data have been imported in the WT sFSPNm with the help of database arcs via the 8760×1 $\boldsymbol{W}$ data vector. This vector is composed of hourly values of the wind speed measurements for the year 2005 from a mountain-placed anemometer in Chania region, Crete. In all simulations, $\boldsymbol{W}$ data vector remains unchanged. The anemometer height is considered to be 10 m, whereas the WT hub height was set equal to 35 m. The wind speed at hub height is then calculated with the help of the power law

$$V(z_{hub}) = V(z_{anem}) \left(\frac{z_{hub}}{z_{anem}} \right)^a \tag{3}$$

where z_{hub} is the hub height of WT, z_{anem} the anemometer height, a the power-law exponent that is set equal to 1/7, $V(z_{hub})$ the wind speed at hub height and $V(z_{anem})$ the wind speed at the anemometer height. Moreover, a forced outage rate of 4% for WT has been considered, with mean time to failure (MTTF) equal to 1920 h and mean time to repair (MTTR) equal to 80 h [3]. For both cases, the probability of time to failure (TTF) and time to repair (TTR) follows an exponential distribution, so both variables can be calculated as follows

$$\text{TTF} = -\text{MTTF} \cdot \ln(\text{rnd}(0, 1)) \tag{4}$$

$$\text{TTR} = -\text{MTTR} \cdot \ln(\text{rnd}(0, 1)) \tag{5}$$

where rnd(0, 1) is the uniformly distributed random

doi: 10.1049/iet-rpg:20070012

Table 1 Initial values of input layer places

Place	Description	Type	Initial value (base scenario)
p_{i1}	number of simulation years	D	100
p_{i2}	hour of the year	D	8760
p_{i3}	day of the year	D	1
p_{i4}	annual peak load demand	C	20.00 kW
p_{i5}	number of WTs	D	1
p_{i6}	rated power of WT, P_R	C	20.00 kW
p_{i7}	hub height of WT	C	35.00 m
p_{i8}	power-law exponent	C	0.143
p_{i9}	cut-in speed of WT, V_{in}	C	3.00 m/s
p_{i10}	cut-out speed of WT, V_{out}	C	24.00 m/s
p_{i11}	mean time to failure for WT	D	1920 h
p_{i12}	mean time to repair for WT	D	80 h
p_{i13}	maximum power of CDG	C	15.00 kW
p_{i14}	minimum allowable load of CDG, as a percentage of its maximum power	C	0.30
p_{i15}	load margin that the WT power has to exceed in order to stop CDG operation	C	0.10
p_{i16}	scheduled maintenance of CDG	D	150 h of operation
p_{i17}	lower bound of CDG maintenance duration	D	1 h
p_{i18}	upper bound of CDG maintenance duration	D	7 h
p_{i19}	starting failure probability of CDG	C	0.04

number generation function in the interval (0, 1). After the calculation of TTF and TTR, the obtained values are rounded down to the nearest integer.

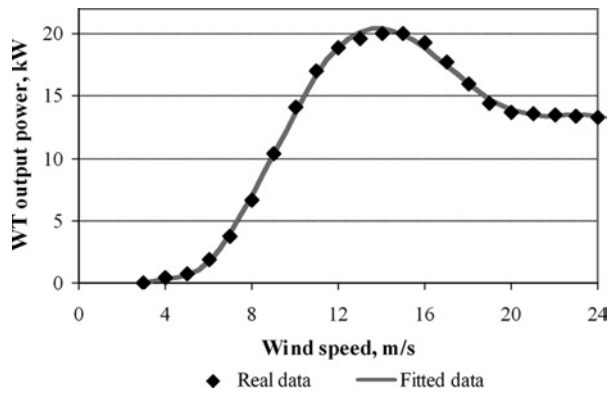

Figure 4 *Correlation between real and fitted data of power curve*

The proposed sFSPNm is depicted in Fig. 5. For each hour, the imported wind speed via database arc at anemometer height of p_{w1} is converted to wind speed at hub height in p_{w3} using (3), and the obtained value is transferred to p_{w6} and p_{w7}. These places are used for finding the WT power-curve section that corresponds to the calculated wind speed when the WT is not in repairing condition. More specifically, p_{w6} and its output test arcs are used for the inspection of the lower bound of WT power-curve section, whereas p_{w7} and its output inhibitor arcs are used for the inspection of the upper bound of WT power-curve section. Firing of t_{w4}, t_{w5} or t_{w6} denote WT power production if $V < V_{in}$, $V_{in} \leq V < V_{out}$ or $V \geq V_{out}$, respectively. The produced WT energy is shown in p_{w10} on an hourly basis and in p_{w21} on an annual basis.

The inspection for the operating and repairing states of the WT is performed in the right part of the

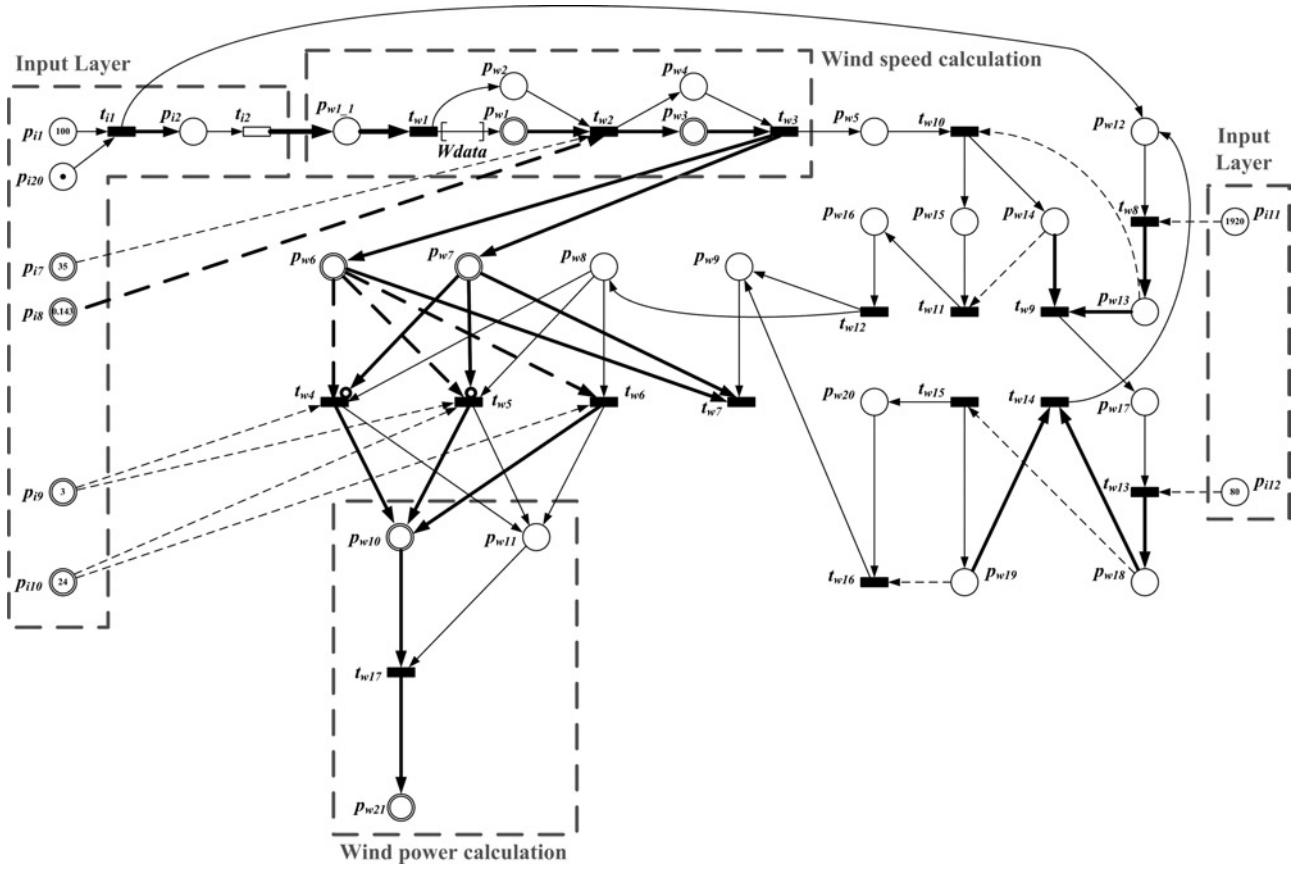

Figure 5 *WT sFSPNm*

sFSPNm in Fig. 5. Places p_{w13} and p_{w18} show the TTF and TTR, respectively. This information is compared with the cumulative time of either operation or repair, which is computed in p_{w14} or p_{w19}, respectively. If the corresponding markings are equal, t_{w9} or t_{w14} fires and activates the opposite WT state (p_{w17} or p_{w12}). If WT is in repair state, p_{w8} is not activated, thus there is no WT power production for the specific hour.

For reader's facility, non-unitary arc weights of the sFSPNm in Fig. 5 are represented in bold. These arc weights are presented in Table 2.

If the number of WTs is greater than 1, different simulations for each WT have to be executed, even if all WTs are of the same type. This occurs because the variation of their corresponding failure and repair durations depends on the random number generation function [(4) and (5)]. The different WTs can be represented by different colours in the sFSPNm of Fig. 5. More specifically, different colours will be used in the part of sFSPNm that included between transitions t_{w3} and t_{w17}. In this case, the arc directed from t_{w17} to p_{w21} will sum the markings of places p_{w10} for all colours.

5.4 Conventional diesel generator sFSPNm

In the CDG sFSPNm, a 15 kW diesel unit is modelled, which needs scheduled maintenance for every 150 h of operation [23]. The lower and upper limits for maintenance duration are set equal to 1 and 7 h, respectively, whereas the corresponding probability distribution is assumed to be uniform. For each simulation hour, the CDG does not operate only if the WT power is larger than the load by some margin, which is considered equal to 10% of the load demand. Moreover, if the CDG operates, its output power cannot be less than a predetermined value, which has been set equal to 30% of the CDG maximum power. Because of the expected large number of start–stop cycles of the conventional generator, a starting failure of 4% is included in the evaluation [24], whereas the repairing process follows the same distribution with the maintenance process.

Fig. 6 presents the structure of the CDG model. The bold arcs have weight different from 1 and their description is presented in Table 3. When the produced energy from WT (place p_{w10}) is greater than the load demand (place p_{l3}) plus a fixed percentage (place p_{i15}) of

doi: 10.1049/iet-rpg:20070012

Table 2 Description of arcs with non-unitary weights in wind turbine sFSPNm

Input	Output	Arc weight
t_{i1}	p_{i2}	8760
t_{i2}	p_{w1_1}	$8761-M_{Pi2}$
p_{w1_1}	t_{w1}	M_{Pw1_1}
p_{w1}	t_{w2}	M_{Pw1}
p_{i8}	t_{w2}	M_{Pi8}
t_{w2}	p_{w3}	$M_{Pw1} * (M_{Pi7}/10)^{M_{Pi8}}$
p_{w3}	t_{w3}	M_{Pw3}
t_{w3}	p_{w6}	M_{Pw3}
t_{w3}	p_{w7}	M_{Pw3}
p_{w6}	t_{w4}	0
p_{w6}	t_{w5}	M_{Pi9}
p_{w6}	t_{w6}	M_{Pi10}
p_{w6}	t_{w7}	M_{Pw6}
p_{w7}	t_{w4}	M_{Pi9}
p_{w7}	t_{w5}	M_{Pi10}
p_{w7}	t_{w7}	M_{Pw7}
t_{w4}	p_{w10}	0
t_{w5}	p_{w10}	$0.00000107 * M_{Pw6}^7 - 0.00012 * M_{Pw6}^6 + 0.00536 * M_{Pw6}^5 - 0.12 * M_{Pw6}^4 + 1.42 * M_{Pw6}^3 - 8.46 * M_{Pw6}^2 + 24.24 * M_{Pw6} - 26.36$
t_{w6}	p_{w10}	0
p_{w10}	t_{w17}	M_{Pw10}
t_{w17}	p_{w21}	M_{Pw10}
t_{w8}	p_{w13}	$-M_{Pi11} * \ln(\text{rnd}(0, 1))$
p_{w13}	t_{w9}	M_{Pw13}
p_{w14}	t_{w9}	M_{Pw13}
t_{w13}	p_{w18}	$-M_{Pi12} * \ln(\text{rnd}(0, 1))$
p_{w18}	t_{w14}	M_{Pw18}
p_{w19}	t_{w14}	M_{Pw18}

the load demand, t_{c2} is enabled and two basic events occur: the information that the CDG does not operate at the specific hour increases by 1 the marking of p_{c27} by the sequential firing of t_{c26} and t_{c27}, whereas the CDG power is set to zero (place p_{c33}) and the excess energy production is calculated in p_{c37}. In the opposite case, the needed power of the CDG is calculated in p_{c2}. If the obtained value is less than the minimum allowable limit, then t_{c4} is enabled and the CDG power is set equal to this limit. Place p_{c4} shows the final acceptable power that the CDG has to give. There are, however, more conditions that have to be examined before the CDG operates. First, the CDG cannot operate if it is already under repair. In this circumstance, p_{c6} has one token and t_{c7} is enabled, leading the model to add zero tokens in CDG's output power place p_{c33}. Secondly, if CDG is not working, the previous hour has to be examined. In this case, p_{c27} will have token(s) and t_{c28} will be enabled, which leads to the inspection of starting failure. Otherwise, t_{c11} will fire, leading to the normal operation of CDG.

Even if the CDG is working properly for a specific hour, an additional constraint has to be examined.

doi: 10.1049/iet-rpg:20070012

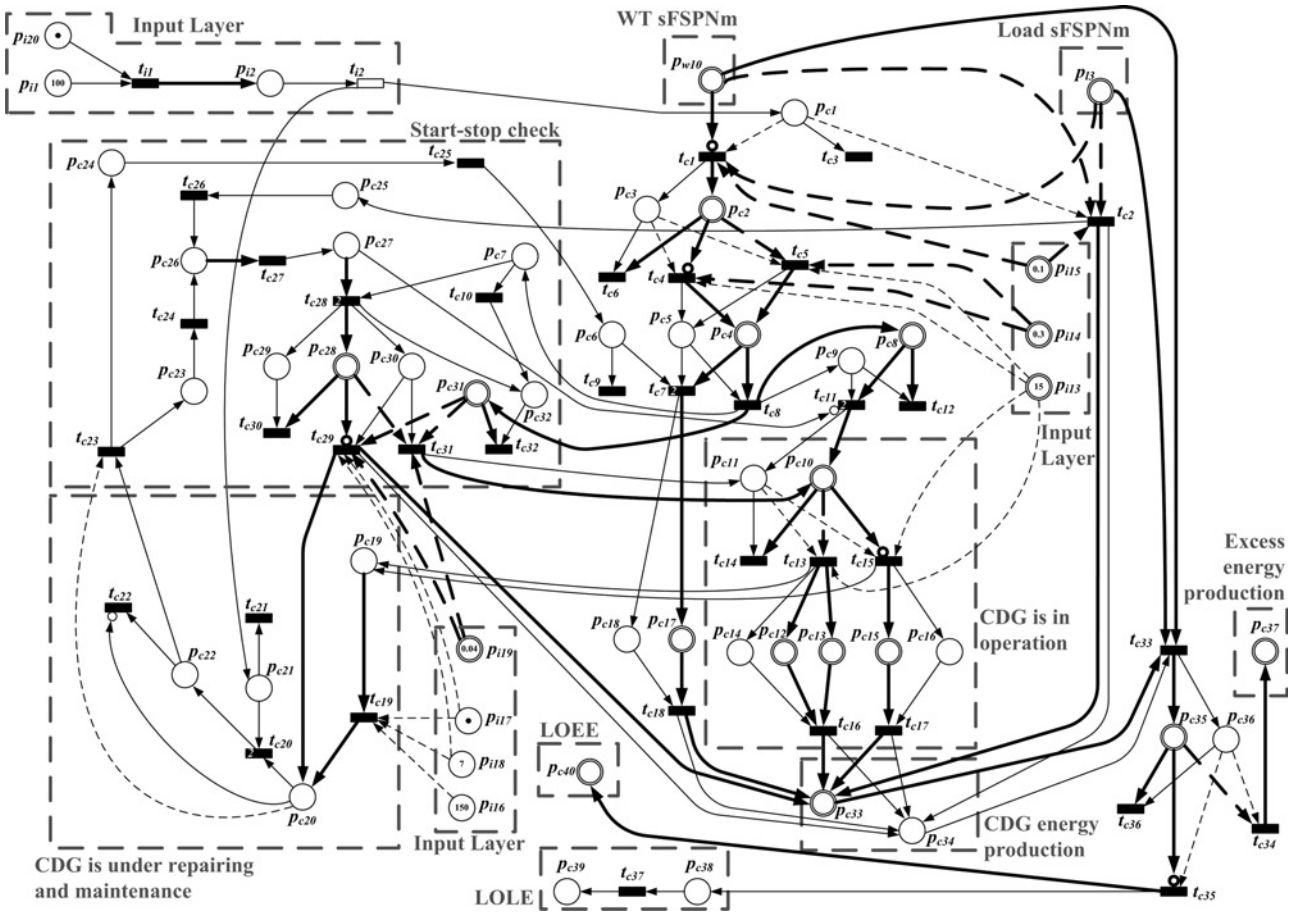

Figure 6 *CDG sFSPNm*

More specifically, if the power that has to be produced by the CDG is greater than the CDG maximum power, the additional power that the generator should serve is calculated at p_{c13}, otherwise all load demand will be satisfied (place p_{c15}). The normal operation of CDG (firing of t_{c13} or t_{c15}) adds one token at p_{c19}. If its marking becomes equal to the duration of CDG scheduled maintenance (place p_{i16}), t_{c19} will be enabled, the duration of CDG repair will be calculated at p_{c20}, and at the end of the process, a token will be added at p_{c27}.

As mentioned earlier, enabling of t_{c28} leads to the examination of CDG starting failure case. A random number is generated at p_{c28} and is compared with the CDG starting failure probability of p_{i19}. If the produced number is greater than the failure probability, the CDG works normally (t_{c31} fires); otherwise t_{c29} is enabled and CDG is in repair, and the procedures followed are identical to those concerning the CDG maintenance procedure after the firing of t_{c19}, described in the previous paragraph.

For each simulation hour, the amount of either SE or unsupplied energy is calculated in p_{c35}, by summing the WT and CDG powers and subtracting the load demand. If the obtained marking is positive, t_{c34} is enabled and the amount of excess electricity production is calculated in p_{c37}; otherwise t_{c35} fires and increases the LOLE marking by one (place p_{c39}) and LOEE marking by the amount of unsupplied energy (place p_{c40}).

5.5 Output layer sFSPNm

The output layer sFSPNm calculates the remaining reliability and performance indices that have not been evaluated in the WT sFSPNm or in the CDG sFSPNm. After the estimation of all indices for the specific year, the simulation procedure is repeated for the next year.

6 Results

In order to investigate the flexibility and the capabilities of the proposed methodology, a base scenario has been considered that is composed of one WT with 20 kW rated power and one CDG with 15 kW rated power. Then the results of the base scenario are compared with the results provided by the same FSPN under the following scenarios: (1) adding more WTs of the same type and (2) installing smaller capacity WTs

IET Renew. Power Gener., 2008, Vol. 2, No. 2, pp. 75–88
doi: 10.1049/iet-rpg:20070012

Table 3 Description of arcs with non-unitary weights in conventional diesel generator sFSPNm

Input	Output	Arc weight
t_{i1}	p_{i2}	8760
p_{w10}	t_{c1}	$M_{Pl3} * (1 + M_{Pi15})$
p_{w10}	t_{c2}	$M_{Pl3} * (1 + M_{Pi15})$
p_{w10}	t_{c33}	M_{Pw10}
p_{l3}	t_{c1}	M_{Pl3}
p_{l3}	t_{c2}	M_{Pl3}
p_{l3}	t_{c33}	M_{Pl3}
p_{i15}	t_{c1}	M_{Pi15}
p_{i15}	t_{c2}	M_{Pi15}
t_{c1}	p_{c2}	$M_{Pl3} - M_{Pw10}$
t_{c2}	p_{c33}	0
p_{c2}	t_{c4}	$M_{Pi14} * M_{Pi13}$
p_{c2}	t_{c5}	$M_{Pi14} * M_{Pi13}$
p_{c2}	t_{c6}	M_{Pc2}
p_{i14}	t_{c4}	M_{Pi14}
p_{i14}	t_{c5}	M_{Pi14}
t_{c4}	p_{c4}	$M_{Pi14} * M_{Pi13}$
t_{c5}	p_{c4}	M_{Pc2}
p_{c4}	t_{c7}	M_{Pc4}
p_{c4}	t_{c8}	M_{Pc4}
t_{c7}	p_{c17}	M_{Pc4}
t_{c8}	p_{c31}	M_{Pc4}
t_{c8}	p_{c8}	M_{Pc4}
p_{c8}	t_{c11}	M_{Pc8}
p_{c8}	t_{c12}	M_{Pc8}
t_{c11}	p_{c10}	M_{Pc8}
p_{c10}	t_{c13}	M_{Pi13}
p_{c10}	t_{c14}	M_{Pc10}
p_{c10}	t_{c15}	M_{Pi13}
t_{c13}	p_{c12}	M_{Pi13}
t_{c13}	p_{c13}	$M_{Pc10} - M_{Pi13}$
t_{c15}	p_{c15}	M_{Pc10}
p_{c12}	t_{c16}	M_{Pc12}
p_{c13}	t_{c16}	M_{Pc13}
p_{c15}	t_{c17}	M_{Pc15}
t_{c16}	p_{c33}	M_{Pc12}
t_{c17}	p_{c33}	M_{Pc15}
p_{c17}	t_{c18}	M_{Pc17}
t_{c18}	p_{c33}	0
p_{c19}	t_{c19}	M_{Pi16}
t_{c19}	p_{c20}	$1 + M_{Pi17} + (M_{Pi18} - M_{Pi17}) * \text{rnd}(0, 1)$
p_{c26}	t_{c27}	M_{Pc26}
p_{c27}	t_{c28}	M_{Pc27}
t_{c28}	p_{c28}	rnd(0, 1)
p_{c28}	t_{c29}	M_{Pi19}
p_{c28}	t_{c30}	M_{Pc28}
p_{c28}	t_{c31}	M_{Pi19}
p_{c31}	t_{c29}	M_{Pc31}
p_{c31}	t_{c31}	M_{Pc31}
p_{c31}	t_{c32}	M_{Pc31}
p_{i19}	t_{c29}	M_{Pi19}
p_{i19}	t_{c31}	M_{Pi19}
t_{c29}	p_{c33}	0
t_{c29}	p_{c20}	$1 + M_{Pi17} + (M_{Pi18} - M_{Pi17}) * \text{rnd}(0, 1)$
t_{c31}	p_{c10}	M_{Pc31}
t_{c33}	p_{c35}	$M_{Pc33} + M_{Pw10} - M_{Pl3}$
p_{c35}	t_{c34}	0
p_{c35}	t_{c35}	0
p_{c35}	t_{c36}	M_{Pc35}
t_{c34}	p_{c37}	M_{Pc35}
t_{c35}	p_{c40}	$-M_{Pc35}$

having the same overall capacity with the WT of the base scenario. To obtain more reliable and accurate results, reliability and performance indices are calculated for a simulation period of 100 years and then averaged.

6.1 Scenario 1: effect of adding same type WTs to the system

Table 4 presents the indices calculated by the FSPN for the case of installing one, two or three WTs of the same

Table 4 Indices for SIPS for three different configurations

Index	One WT (base scenario)	Two WTs	Three WTs
LOLP, %	8.07	5.79	5.03
LOLE, h/year	706.87	507.47	440.53
LOEE, kW h/year	2289.72	1968.37	1 837.39
EIU, %	2.16	1.83	1.71
SI, system min/year	6869	5905	5512
FOI, int/year	239.39	199.48	174.38
DOI, h/int	2.95	2.54	2.53
ENSI, kW h/int	9.57	9.87	10.53
LCI, kW/int	3.24	3.87	4.16
WEP, kW h	56 240	111 845	168 169
CEP, kW h	62 991	50 070	44 318
CF, %	32.16	31.92	31.99
SE, kW h	13 820	56 117	106 624

type (each WT having 20 kW rated power), combined with one CDG of 15 kW. The case with one WT of 20 kW combined with one CDG of 15 kW forms the base scenario.

From Table 4, it is concluded that the addition of a second WT improves significantly the reliability indices and also reduces the use of the CDG. On the other hand, the surplus energy (SE) is increased and it may require the exploitation of this unused amount of energy. The addition of a third WT further improves the performance of the system and increases the SE. The last two scenarios may become very attractive if environmental and financial factors that are not analysed in this paper are taken into account (e.g. subsidies for WT purchase). Power quality issues should also be considered as the penetration of wind power is increased. However, such a detailed analysis is beyond the scope of this paper.

Fig. 7 depicts the evolution of system's loss of energy for the first simulation year. The obtained value in the 8760th hour is equal to the LOEE index for the specific year. It can be noted that the higher the number of WTs, the lower the amount of unsupplied energy for almost every hour of the year. The small violations of the above-mentioned conclusion are explained by the random nature of WT TTF, WT TTR, CDG starting failure and CDG maintenance duration of the specific's year simulation procedure.

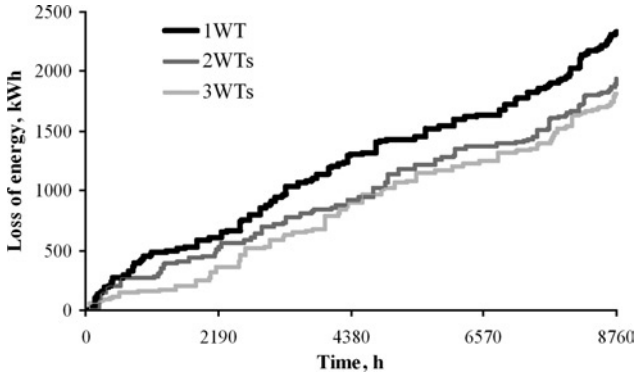

Figure 7 *Loss of energy evolution for the first simulation year*

6.2 Scenario 2: effect of using smaller WTs with same overall rated power

In the second scenario, two WTs of $P_R = 10$ kW are considered, having the same V_{in} and V_{out} with the 20 kW WT of the base scenario. The new power-curve equation can be concluded from (2), by dividing its coefficients by two. As can be seen from Table 5, although the overall energy production of scenario 2 is lower than scenario 1, the better distribution of WTs maintenance procedure improves slightly almost all indices. The fact that the initial cost of one 20 kW WT is lower compared with the initial cost of two 10 kW WTs has also to be considered in the overall decision, using an appropriate methodology that calculates the system's

Table 5 Indices for the base and second scenarios

Index	Base scenario	Second scenario
LOLP, %	8.07	7.73
LOLE, h/year	706.87	677.57
LOEE, kW h/year	2289.72	2231.81
EIU, %	2.16	2.07
SI, system min/year	6869	6695
FOI, int/year	239.39	241.57
DOI, h/int	2.95	2.81
ENSI, kW h/int	9.57	9.25
LCI, kW/int	3.24	3.29
WEP, kW h	56 240	55 848
CEP, kW h	62 991	63 000
CF, %	32.16	31.88
SE, kW h	13 820	13 379

doi: 10.1049/iet-rpg:20070012

overall cost of energy taking into account its initial cost, the energy produced and the penalty cost of the unsupplied energy.

7 Conclusion

The proposed FSPN methodology is very efficient in reliability and performance analysis of hybrid SIPS, since (1) it presents the advantages of simulation methods, (2) it has the additional characteristic of the visualisation of the simulation procedure that makes it a powerful communication medium between theoreticians and practitioners, (3) it represents in the same model the static structure of the system as well as its dynamically changing state and (4) with the use of the proposed database arcs, real data can be easily imported in the simulation process, assuring the validity of the obtained results. The proposed method is general and can be applied to a wide range of power systems types. In addition, with rather few alterations and additions, the use of the described methodology may be further generalised to study systems from areas with similar characteristics. From the presented analysis and discussion of the results, it has been shown that the proposed FSPN methodology is a very promising tool in reliability and performance evaluation of SIPS.

8 Acknowledgments

This work has been performed within the European Commission (EC)-funded VBPC-RES project (contract number FP6-INCO-CT-2004-509205). The authors wish to thank the VBPC-RES partners for their contribution and the EC for partially funding this project.

9 References

[1] KARKI R, BILLINTON R: 'Reliability/cost implications of PV and wind energy utilization in small isolated power systems', *IEEE Trans. Energy Convers.*, 2001, **16**, (4), pp. 368–373

[2] BILLINTON R, ALLAN RN: 'Reliability evaluation of power systems' (Plenum Press, 1984)

[3] KARKI R, BILLINTON R: 'Cost effective wind energy utilization for reliable power supply', *IEEE Trans. Energy Convers.*, 2004, **19**, (2), pp. 435–440

[4] BILLINTON R, BAGEN YC, CUI Y: 'Reliability evaluation of small stand-alone wind energy conversion systems using a time series simulation model', *IEE Proc., Gener. Transm. Distrib.*, 2003, **150**, (1), pp. 96–100

[5] MURATA T: 'Petri nets: properties, analysis and applications', *Proc. IEEE*, 1989, **77**, (4), pp. 541–580

[6] JENSEN K: 'An introduction to the theoretical aspects of coloured Petri nets', *Lect. Notes Comput. Sci.*, 1994, **803**, pp. 230–272

[7] DAVID R, ALLA H: 'Petri nets for modeling of dynamic systems – a survey', *Automatica*, 1994, **30**, (2), pp. 175–202

[8] TSINARAKIS GJ, TSOURVELOUDIS NC, VALAVANIS KP: 'Modeling, analysis, synthesis, and performance evaluation of multioperational production systems with hybrid timed Petri nets', *IEEE Trans. Autom. Sci. Eng.*, 2006, **3**, (1), pp. 29–46

[9] TRIVEDI KS, KULKARNI VG: 'FSPNs: fluid stochastic Petri nets'. 14th Int. Conf. Applications and Theory of Petri Nets, 1993, pp. 24–31

[10] TUFFIN B, CHEN DS, TRIVEDI KS: 'Comparison of hybrid systems and fluid stochastic Petri nets', *Discrete Event Dyn. Syst., Theory Appl.*, 2001, **11**, pp. 77–95

[11] LIN C-H: 'Distribution network reconfiguration for load balancing with a coloured Petri net algorithm', *IEE Proc., Gener. Transm. Distrib.*, 2003, **150**, (3), pp. 317–324

[12] GEORGILAKIS PS, KATSIGIANNIS JA, VALAVANIS KP, *ET AL.*: 'A systematic stochastic Petri net based methodology for transformer fault diagnosis and repair actions', *J. Intell. Robot. Syst.*, 2006, **45**, pp. 181–201

[13] LU N, CHOW JH, DESCROCHERS AA: 'A multi-layer Petri net model for deregulated electric power systems'. Proc. American Control Conf., 2002, pp. 513–518

[14] SALEFHAR H, LI T: 'Stochastic Petri nets for reliability assessment of power generating systems with operating considerations'. IEEE Power Engineering Society 1999 Winter Meeting, 1999, pp. 459–464

[15] DUMITRESCU M: 'Stochastic Petri nets architectural modules for power system availability', *Proc. Electron. Circuits Syst.*, 2002, **2**, pp. 745–748

[16] IEEE: 'The IEEE reliability test system', 1996

[17] LIPMAN NH: 'Overview of wind/diesel systems', *Renew. Energy*, 1994, **5**, (I), pp. 595–617

[18] ACKERMANN T: 'Wind power in power systems' (Wiley, 2005)

[19] CIARDO G, NICOL DM, TRIVEDI S: 'Discrete-event simulation of fluid stochastic Petri nets', *IEEE Trans. Softw. Eng.*, 1999, **25**, (2), pp. 207–217

[20] Available at: http://www.nrel.gov/homer, accessed September 2007

[21] Available at: http://www.ceere.org/rerl/projects/software/hybrid2/download.html, accessed September 2007

[22] Available at: http://www.r-drath.de/VON/von_e.htm, accessed September 2007

[23] MUSELLI M, NOTTON G, LOUCHE A: 'Design of hybrid-photovoltaic power generator, with optimization of energy management', *Sol. Energy*, 1999, **65**, (3), pp. 143–157

[24] BAGEN YC, BILLINTON R: 'Evaluation of different operating strategies in small stand-alone power systems', *IEEE Trans. Energy Convers.*, 2005, **20**, (3), pp. 654–660

doi: 10.1049/iet-rpg:20070012